International Journal of Automotive Technology, Vol. 16, No. 4, pp. 629–634 (2015)
DOI 10.1007/s12239–015–0064–8

pISSN 1229–9138/ eISSN 1976–3832

DESIGN OF REAR GLASS-INTEGRATED ANTENNAS WITH VERTICAL LINE OPTIMIZATION FOR FM RADIO RECEPTION

G. BYUN[1)], Y. G. NOH[2)], I. M. PARK[3)] and H. S. CHOO[4)*]

[1)]Department of Electronics and Computer Engineering, Hanyang University, Seoul 133-791, Korea
[2)]Corporate Research & Development Division, Hyundai-Kia Motors, 150 Hyundaiyeonguso-ro, Namyang-eup, Hwaseong-si, Gyeonggi 445-869, Korea
[3)]School of Electrical and Computer Engineering, Ajou University, Gyeonggi 443-749, Korea
[4)]School of Electronic and Electrical Engineering, Hongik University, Seoul 121-791, Korea

(Received 1 December 2012; Revised 26 September 2013; Accepted 18 September 2014)

ABSTRACT–We propose an glass-integrated antenna with vertical lines for FM radio reception in a commercial sedan. The proposed antenna consists of vertical lines and multiple horizontal lines that are also used as defroster lines. The proposed antenna structure is optimized with the genetic algorithm (GA) in conjunction with the FEKO EM simulator. The optimized antenna was built and installed on an Azera test vehicle (Korean model: TG Grandure 270) from Hyundai-Kia Motors and antenna performances such as reflection coefficients, and bore-sight gain are measured in an anechoic chamber. The optimized antenna shows a half power matching bandwidth of 26 % at the center frequency of the FM radio band and an average bore-sight gain of about -10.37 dBi. Then, we performed a field test to measure actual received power of FM radio signals. The field test result shows that the proposed antenna is capable of maintaining higher received power levels compared to the conventional antenna for both the strong and weak signals in the real urban situation.

KEY WORDS : Vehicle antennas, Glass-integrated antennas, FM antennas

1. INTRODUCTION

In recent years, glass-integrated antennas have gained their popularity in many vehicular applications, such as FM/AM radio reception, digital multimedia broad casting (DMB), wireless broadband (WiBro) communications, and high-speed downlink packet access (HSDPA). These antennas are aerodynamic and visually appealing because the antenna lines are directly printed on the inner surface of rear windshields (Batchelor *et al*., 2001; Noh *et al*., 2005; Low *et al*., 2006). The improved aerodynamic characteristics allow the antenna to have a better performance in terms of durability and wind noise characteristics that have been discussed as disadvantages of roof-top antennas. However, there are some critical design considerations for glass-integrated antennas; first, the antenna structure should be simple and visually transparent for the driver's field of view. Second, the antenna should have broad matching bandwidth with high radiation gain that are usually degraded by a high dielectric constant ($\varepsilon_r = 6.85$) and a high loss tangent ($tan\delta = 0.05$) of the glass material (Abou-Jaoude and Walton, 1998; Ahn and Choo, 2010). In addition, a relatively high resistance (approximately 0.5 Ω/m) of the horizontal lines, that are simultaneously used as defroster lines, should be taken into account in our design process since it lowers the radiation efficiency. An omni-directional property is also an important design consideration for FM radio reception because the antenna is placed in close proximity to the conducting frame, which causes the body blockage effect degrading the omni-directional property (Josefsson and Persson, 2006). The vertical gain is important in vehicular FM radio reception, because the vertically polarized component is dominant in the transmitted FM radio signals. To satisfy these considerations, a commercial FM antenna, that is currently used for FM radio reception, contains fifteen horizontal defroster lines with two vertical lines that are adopted to raise the antenna vertical gain by inducing more vertical currents (Balanis, 2005; Felsen and Marcuvitz, 1994).

In this paper, we propose a rear glass-integrated antenna with vertical lines to maximize the vertical gain for FM radio reception on a commercial sedan. First, we establish appropriate EM simulation conditions to achieve both high accuracy and fast simulation time by adjusting the mesh number. We also verify the importance of the starting point of vertical lines with current distributions and observe the performance changes according to the vertical line widths to further improve the antenna gain. Based on the findings, we design a glass-integrated antenna using vertical lines

**Corresponding author*. e-mail: hschoo@hongik.ac.kr

and optimize the antenna structure by changing the number, position, length, angle, and line width of the vertical lines. We limit the number of vertical lines up to 5 to guarantee a clear field of view for a driver. A genetic algorithm (GA) is used to optimize the antenna performance in conjunction with the FEKO EM simulator (FEKO Suite 6.1, EM software and Systems; Goldberg, 1989; Rahmat-Samii and Michielssen, 1999). To verify antenna performance, the optimized antenna is built and installed on our Azera test vehicle (Korean model: TG Grandure 270) from Hyundai-Kia Motors (Hyundai Grandeur TG Q 240, 2007). Then, we conduct an indoor and outdoor test to evaluate the antenna performance such as a matching characteristic, radiation gain, and the reception capability. The test results demonstrate that the optimized antenna is suitable for an FM antenna to use in vehicles.

2. EM SIMULATION AND DESIGN MOTIVATION

Figure 1 shows a rear view of a vehicle (Azera, Korean model: TG Grandure 270) from Hyundai-Kia Motors; the glass-integrated antenna is placed on the rear windshield. As specified in the figure, the feed position is located on the left side of the windshield, and a wire port is adopted for the antenna excitation. Since the length of the vehicle body is approximately one wavelength of the FM radio frequency band, input impedances and radiation patterns are significantly affected by a specific geometry of the vehicle, such as vehicle frames and interior parts. Therefore, we include the entire geometry in the EM simulator as piece-wise mesh triangles and find the most appropriate number of triangles by considering both the simulation time and accuracy. As a result, the entire geometry is remodeled as 4,600 piece-wise mesh triangles to obtain a simulation time of less than 2 minutes for each frequency point with the simulation accuracy of greater than 80% compared to the 16,000 piece-wise triangles (an average edge length: approximately λ/30 at 88 MHz).

The design parameters of the horizontal defroster lines are pre-determined by considering the shape of the rear

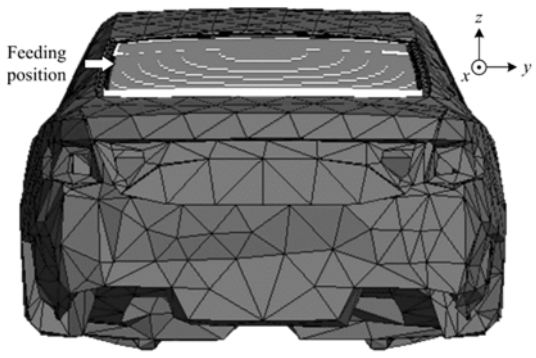

Figure 1. Geometry of the vehicle.

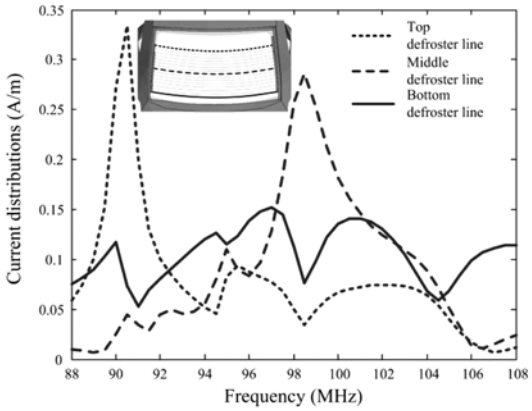

Figure 2. Current distributions of horizontal defroster lines vs. frequency.

wind shield. Thus, we give more design freedom to the antenna by inserting vertical lines. Since the vertical lines are useful to spread the segment currents to the entire antenna structure by connecting horizontal lines, current distributions are usually denser near the intersecting points between vertical and horizontal lines. To find the proper positions of the vertical lines, we first examine the segment current distributions of the horizontal-line-only antenna to determine the placement of the vertical lines and to examine how the vertical lines effectively affect the vertical gain of the antenna. Figure 2 shows induced current distributions at the top, middle, and bottom horizontal lines over the frequency range. The top line shows a peak value of approximately 0.33 A/m at 91 MHz with the average current distribution of 0.07 A/m over the range. A peak value is found at 99 MHz in the middle line, whose average current distribution is approximately 0.08 A/m. The bottom line, however, shows relatively uniform current distributions in the entire range with an average value of 0.11 A/m, which is the greatest value among the simulated lines. Then, we insert three vertical lines that are originated from each of the top, middle, and bottom

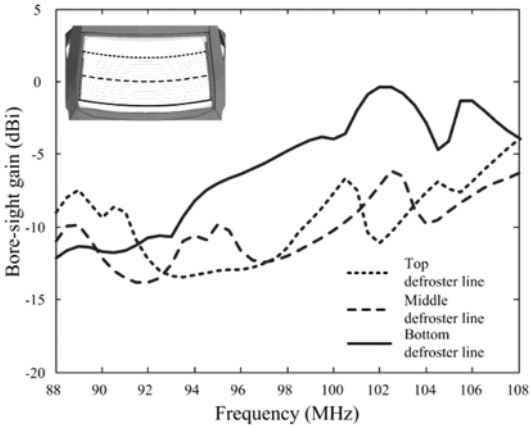

Figure 3. Bore-sight gain vs. orientation of vertical lines.

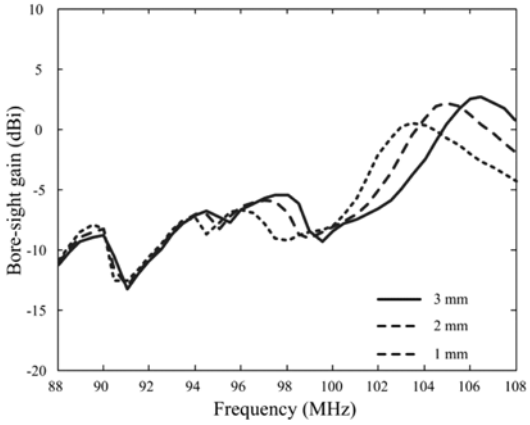

Figure 4. Vertical gain vs. vertical line widths.

horizontal lines, and they connect five closest horizontal lines from their origins. Figure 3 shows a comparison of vertical gains in the bore-sight direction (x-axis, $\phi = 0^{o}$) according to the originating horizontal lines. The result shows that the average gain is improved by 0.42 dB, when the vertical lines are originated from the bottom line. In other words, higher average current distributions can improve vertical bore-sight gain by supplying more vertical currents to the vertical lines (Kand and Choo, 2010).

To further verify whether the vertical gain can be improved by the width, we observe the performance Variation when the vertical line width varies from 1 mm to 3 mm. Figure 4 shows a comparison of the vertical gain as a function of frequency with an assumption that three vertical lines are originated from the bottom defroster line. The results illustrate that a wider width improves the vertical gain, especially in the higher frequency band, which is achieved by less resistive line impedance.

We also verified the importance of other design parameters, such as lengths, angles, and positions, and found out that they were also sensitive to the vertical gain. Thus, those parameters were considered as important design factors in our optimization process.

3. ANTENNA STRUCTURES AND OPTIMIZATION

Figure 5 (a) shows a top view of the proposed antenna structure, which consists of existing horizontal defroster lines and vertical lines, and the antenna structure is printed on the inner surface of the rear windshield (thickness = 3 mm, $\varepsilon_r = 6.85$, $tan\delta = 0.05$). Horizontal lines are placed at intervals of 30 mm, and their line width is fixed at 1 mm, as shown in Figure 5 (b). The vertical lines originate from the bottom horizontal line and are determined to connect the horizontal lines with their lengths (L_1, L_2, and L_3), angles (α_1, α_2, and α_3), positions (D_1, D_2, and D_3), and widths (W_1, W_2, and W_3).

To further improve the vertical gain as well as the

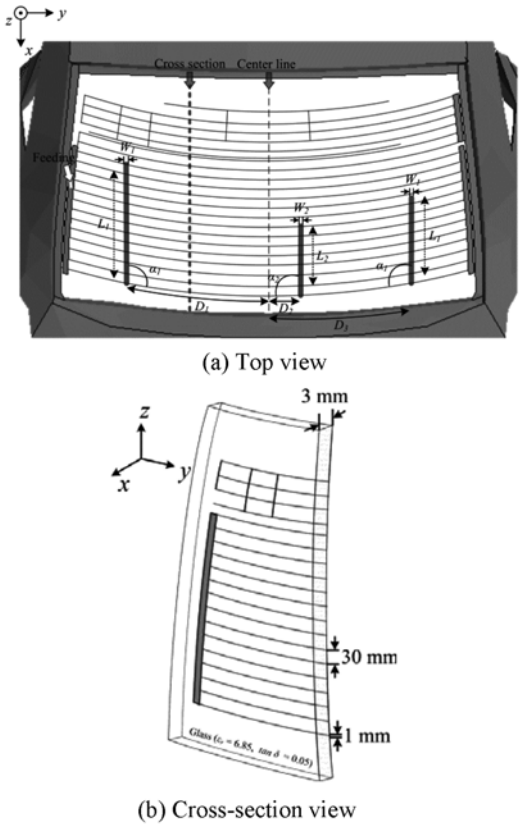

(a) Top view

(b) Cross-section view

Figure 5. The proposed antenna structure.

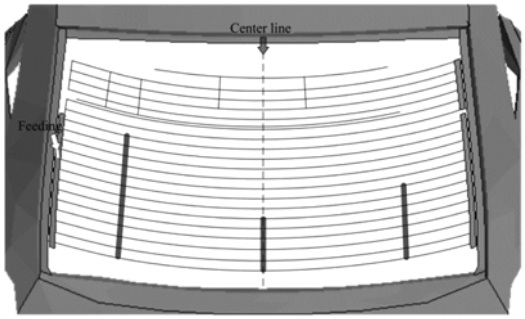

Figure 6. Optimized antenna structure.

impedance matching characteristics, the proposed antenna structure is optimized by the GA in conjunction with the FEKO EM simulator. In our GA process, we vary the lengths from 30 mm to 420 mm and the angles from 85° to 95°. We determined the initial values of the vertical lines to be about a quarter wavelength at 98 MHz (Milligan, 2005), and then, symmetrically place the vertical lines with respect to the center of the horizontal defrost lines. The number of vertical lines (N) is limited to three, and the width is limited to 3 mm in order to guarantee the driver's field of view as clear as possible.

Equation (1) shows cost functions that we used in our

optimization. The first cost function is defined to raise the vertical gain and is determined by the reciprocal of the minimum vertical bore-sight gain ($G_{ver.bore\text{-}sight}$) in the FM radio band (88 MHz–108 MHz). The second cost shows the maximum pattern deviation in the azimuth direction and is defined to minimize the pattern distortions for omni-directional properties. Since the shape of the vertical lines is determined by using twelve design parameters, our optimization process can be considered as a 12-dimensional problem.

$$\begin{aligned} \text{Cost 1} &= \frac{1}{\min\{G_{ver.bore-sight}(f)\}} \\ \text{Cost 2} &= \max[\max\{G_{ver.}(f)\} - \min\{G_{ver.}(f)\}] \\ &\text{, where 88 MHz} < f < 108 \text{ MHz} \end{aligned} \tag{1}$$

The process stops when the minimum vertical bore-sight gain is greater than −10 dBi (Cost 1 < 0.1), and the pattern deviation is less than 20 dB (Cost 2 < 100). The optimized design was obtained after 13 generations, each of which consisted of 30 populations. Thus, the total running time of about 90 hours was spent on a computer with an Intel Core 2 quad-core processor and 4 GB of RAM. Figure. 6 shows the optimized antenna structure, and the detailed parameters are shown in Table 1. The antenna contains three vertical lines that are symmetrically placed with respect to the center vertical line, and the vertical line widths of the antenna are thicker than the horizontal lines so as to increase the vertical gain.

Table 1. Optimized antenna parameters.

Parameters	Values
N	3
L_1 (mm)	342.3
L_2 (mm)	147.5
L_3 (mm)	199.7
W_1 (mm)	3.0
W_2 (mm)	2.3
W_3 (mm)	2.8
D_1 (mm)	440.8
D_2 (mm)	0.0
D_3 (mm)	440.8
α_1 (°)	91.7
α_2 (°)	90.0
α_3 (°)	92.3

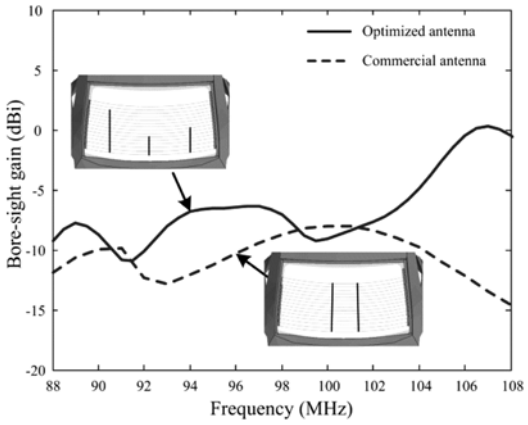

Figure 7. A comparison of vertical bore-sight gains.

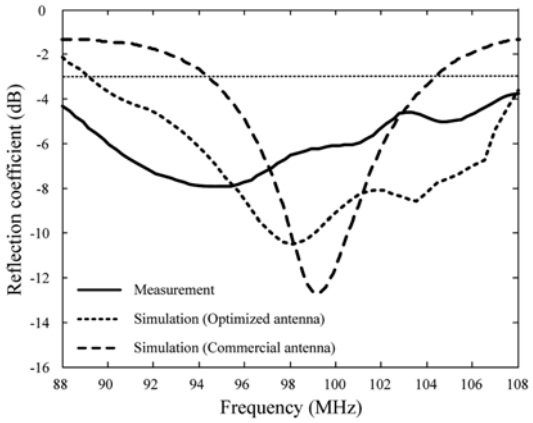

Figure 8. Reflection coefficient of the optimized antenna in comparison with the conventional antenna.

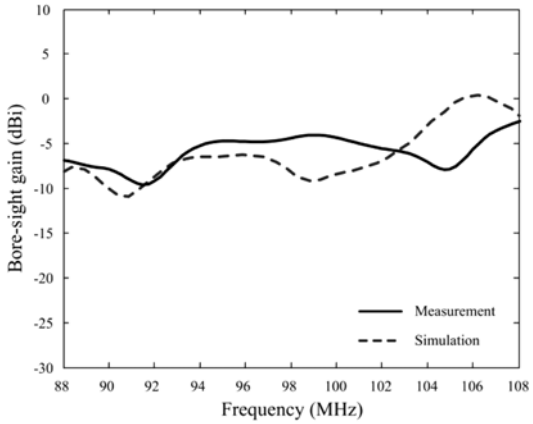

Figure 9. Vertical bore-sight gain of the optimized antenna.

Figure 7 shows the vertical bore-sight gain of the antenna in comparison with that of the conventional antenna having two vertical lines. As can be seen, the average vertical gain of the antenna is improved by 6.1 dB in the FM radio frequency band.

4. MEASUREMENT AND EVALUATION

To verify the antenna performance, the optimized antenna was built and installed on our Azera test vehicle, and its characteristics were measured in an anechoic chamber that

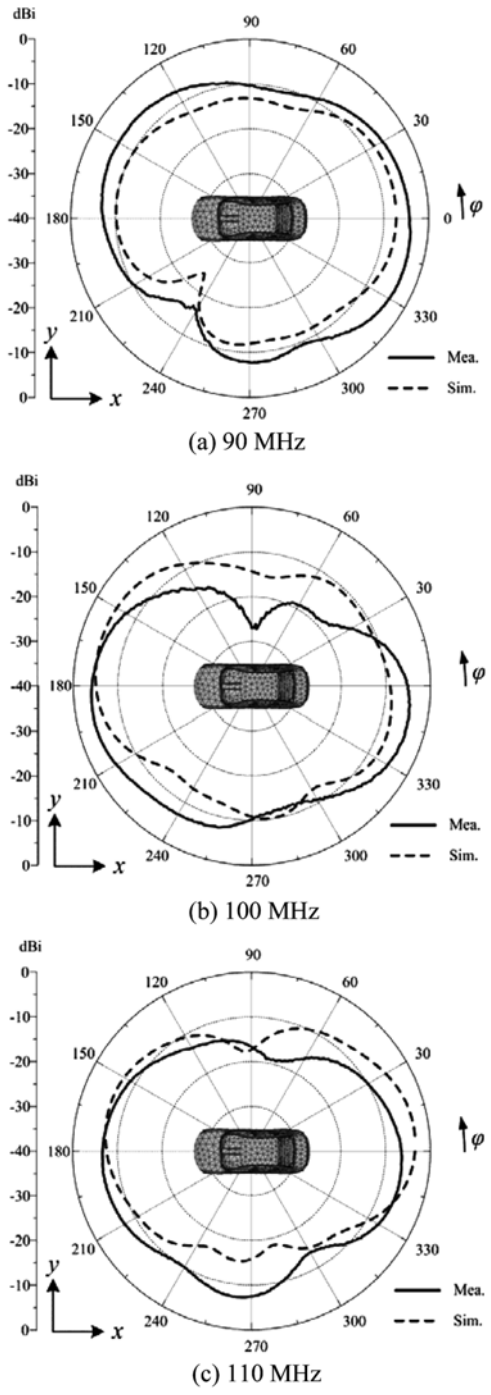

Figure 10. Radiation pattern of the optimized antenna.

is large enough to place the real vehicle inside. Figure 8 shows the measured and simulated reflection coefficients of the optimized antenna. The measured result shows a half power bandwidth (HPBW) of 26% ($|\Gamma| < 3$dB, 87 MHz – 113 MHz), which was improved by 16% compared to the conventional antenna whose fractional HPBW is 10% ($|\Gamma| < 3$dB, 94 MHz – 104 MHz) at 99 MHz. The deviation between the simulation and the measurement was occurred

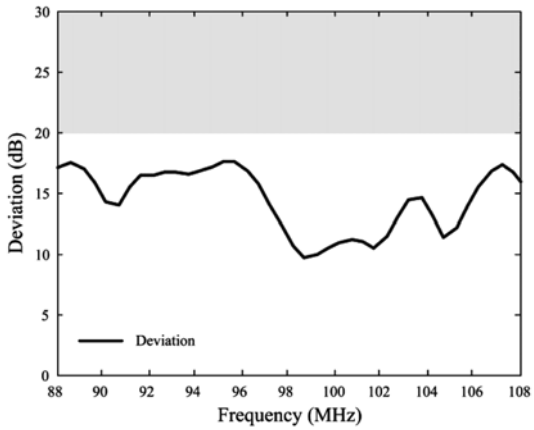

Figure 11. Deviation of azimuth patterns.

by the interior materials placed in close proximity to the antenna, because they were not taken into consideration in our EM simulation due to high computational loads. Figure 9 presents the measured bore-sight gain of the antenna as a function of frequency. The figure shows that the antenna has a minimum gain of greater than −15 dBi in the entire FM band with an average gain of −10.37 dBi.

To examine omni-directional properties of the antenna, radiation patterns were measured at 90 MHz, 100 MHz, and 110 MHz, as shown in Figure 10 (a), (b), and (c), respectively. As can be seen, the radiation gain is stronger in the front and rear directions than the side direction, which is distorted by conducting frames of the vehicle. The radiation gain, averaged over the azimuth direction, exceeds −15 dBi at the three frequency points, and the measured pattern deviations are calculated as 15.80 dB, 10.54 dB, and 15.06 dB, respectively. Figure 11 shows the simulated deviation along the azimuth direction, which is conducted to further examine the antenna's omni-directional properties. The figure shows an average deviation value of approximately 14.5 dB in the entire band, which can be considered as omni-directional patterns, considering the

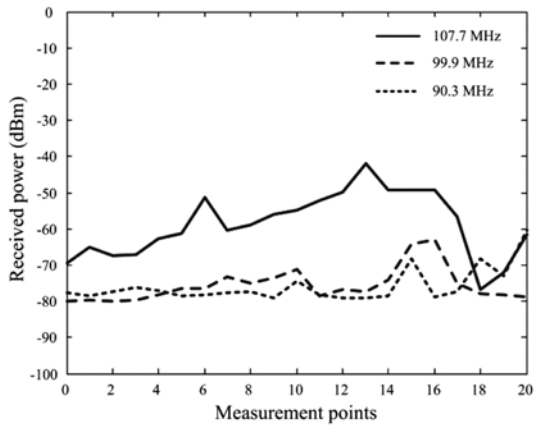

Figure 12. Measured received power.

Table 2. Signal transmitters.

Frequency (MHz)	107.7	99.9	90.3
Trans. Power (kW)	10	5	1
Distance (km)	12	23	50

body blockage effect caused by conducting frames of such a large structure considering the wavelength.

A field test was then conducted to measure received powers of the real FM radio signals to demonstrate how the antenna operates functionally in a real urban situation, where both strong and weak FM radio signals coexist. The measurement was performed in a moving vehicle with a spectrum analyzer installed in our test sedan. The test site, Namsan in the Jung-gu district, Seoul, Korea, was carefully selected considering the field strengths of various FM radio signals. For example, the signal from the 107.7 MHz transmitter shows a relatively strong field strength, while both the 99.9 MHz and 90.3 MHz transmitters have weaker field strengths in Namsan. Table 2 shows more information of the signal transmitters such as transmitting frequencies, powers, and distances from the location where the field test took place. Figure 12 shows received powers measured while the vehicle was running at a speed of 30 km/h on a 4-km road. The antenna shows average received powers of approximately −60 dBm (107.7 MHz), −76 dBm (99.9 MHz), and −78 dBm (90.3 MHz), which are higher than those of the conventional antenna with −74 dBm (107.7 MHz), −75 dBm (99.9 MHz), and −79 dBm (90.3 MHz). The measured data demonstrate that the antenna is capable of maintaining higher received power levels compared to the conventional antenna for both the strong and weak signals in the real urban situation (Ahn *et al*., 2010).

5. CONCLUSION

In this paper, we proposed the design of rear glass-integrated antennas with vertical lines for FM radio reception. The proposed antenna structure was composed of horizontal defroster lines and vertical lines originated for the bottom defroster line. The antenna structure was printed on the inner surface of the rear windshield. The number of vertical lines (N) was limited to 3, and the width was limited to 3 mm in order to guarantee the driver's field of view remained as clear as possible. Then, the proposed antenna structure was optimized by changing the vertical lines' positions, lengths, angles, and widths by using the GA in conjunction with the FEKO EM simulator. The optimized antenna showed a HPBW of about 26% at the center frequency of the FM radio band. The antenna showed an average bore-sight gain of −10.37 dBi in the FM band, and radiation patterns along the azimuth direction showed omni-directional properties with pattern deviations of less less than 15 dB. To evaluate the reception capabilities, a field test was conducted at Namsan in the Jung-gu district, Seoul, Korea while the vehicle was running at a speed of 30 km/h on a 4-km road. The field test results showed that the proposed antenna is capable of maintaining higher received power levels compared to the conventional antenna for both the strong and weak signals in the real urban situation.

ACKNOWLEDGEMENT−This research was supported by the MSIP (Ministry of Science, ICT&Future Planning), Korea, under the ITRC (Information Technology Research Center) support program (NIPA-2013-H0301-13-2007) supervised by the NIPA (National IT Industry Promotion Agency).

REFERENCES

Abou-Jaoude, R. and Walton, E. K. (1998). Numerical modeling of on-glass conformal automobile antennas. *IEEE Trans. Antennas Propag.* **46**, **6**, 845−852.

Ahn, S. and Choo, H. (2010). A systematic design method of on-glass antennas using mesh-grid structures. *IEEE Trans. Veh. Technol.* **59**, **7**, 3286−3293.

Ahn, S., Park, S., Noh, Y., Park, D. and Choo, H. (2010). Design of an glass-integrated vehicle antenna using a multiloop structure. *Microwave and Optical Technology Letters* **52**, **1**, 107−110.

Balanis, C. A. (2005). *Antenna Theory: Analysis and Design.* 3rd edn. Wiley. New York.

Batchelor, J. C., Langley, R. J. and Endo, H. (2001). Glass-integrated mobile antenna performance modeling. *IEE Proc. Inst. Elect. Eng. Microwave Antennas Propag.* **148**, **4**, 233−238.

FEKO Suite 6.1 (2012). EM Software and Systems. http://www.feko.info

Felsen, L. B. and Marcuvitz, N. (1994). *Radiation and Scattering of Waves*. 2nd edn. IEEE Press. New York.

Goldberg, D. E. (1989). *Genetic Algorithms in Search, Optimization and Machine Learning. Reading.* Addison-Wesley. Boston.

Hyundai Grandeur TG Q 240 (2007). http://www.hyundai.com/

Josefsson, L. and Persson, P. (2006). *Conformal Array Antenna Theory and Design*. John Wiley & Sons Inc. New York.

Kang, W. and Choo, H. (2010). Design of vertical lines for vehicle rear window antennas. *Microwave and Optical Technology Letters* **52**, **6**, 1445−1449.

Low, L., Langley, R., Breden, R. and Callaghan, P. (2006). Hidden automotive antenna performance and simulation. *IEEE Trans. Antennas Propag.* **54**, **12**, 3707−3712.

Milligan, T. A. (2005). *Modern Antenna Design.* 2nd edn. John Wiley & Sons. IEEE Press.

Noh, Y., Kim, Y. and Ling, H. (2005). Broadband on-glass antenna with mesh-grid structure for automobiles. *Electron. Lett.* **41**, **21**, 1148−1149.

Rahmat-Samii, Y. and Michielssen, E. (1999). *Electromagnetic Optimization by Genetic Algorithms*. Willey. New York.